




A Methodology for Experimental Quantification of Firebrand Generation from WUI Fuels

Mohammadhadi Hajilou, Steven Hu and Thomas Roche, Department of Fire Protection Engineering, University of Maryland, College Park 3106 J.M. Patterson Building, 4356 Stadium Drive, College Park, Maryland, MD 20742-3301, USA

Priya Garg and Michael J. Gollner , Department of Mechanical Engineering, University of California, Berkeley 6141 Etcheverry Hall, Berkeley, CA 94720-1740, USA

Received: 23 June 2020/**Accepted:** 9 March 2021/**Published online:** 20 April 2021

Abstract. Over the past few years, numerous large-scale disasters have occurred due to wildfires at the wildland-urban interface (WUI). In these fires, spread via the transport of firebrands (burning embers) plays a significant role. Several models have been developed to describe the transport of firebrands but few, if any, are available which can provide a quantitative means to generate firebrands at the source of a fire. In this regard, a new methodology is proposed here that uses a wind tunnel to experimentally quantify the generation of firebrands from WUI fuels under different ambient conditions. The setup allows for the collection of all generated solid firebrands and major downstream gaseous species concentrations. Unique firebrand yield correlations can then be generated for each tested fuel, while also accounting for the heat-release rate, providing unique validation targets for numerical simulations. Generation of firebrands from branches of two conifers at a fixed wind speed of 4 m/s are presented to demonstrate the capabilities of this new methodology. A carbon mass balance was utilized to analyze preliminary results and understand how much of the fuel mass transitions to firebrands vs. gases. These results provide a description of the mass burning process and ultimately tie firebrand production to a time-dependent heat-release rate for initialization of firebrand transport in numerical simulations. An average firebrand yield ranging from 3–4% of initial dry mass is ultimately presented for lodgepole pine and Douglas fir. Future work is required with larger fuel sizes pertaining to real wildfire scenarios; however, the presented methodology can provide valuable data needed to initialize numerical simulations of firebrand transport, necessary for reconstruction of WUI fires and to aid in the development of mitigation strategies for the prevention of future disasters.

Keywords: Firebrand Generation, Wildland Urban Interface (WUI), Wildland Fire, Vegetative Fuels

*Correspondence should be addressed to: Michael J. Gollner, E-mail: mgollner@berkeley.edu



1. Introduction

The number of devastating wildland fires, particularly at the wildland-urban interface (WUI), have increased dramatically over the past few decades [1–3]. A recent example was the destructive 2018 Camp fire killing 85 civilians and destroying almost 18,000 structures around the town of Paradise, California [4]. It is expected that this trend will continue due to climate change, increased movement of populations into rural areas, and suboptimal fire management policies. Improved understanding of fire spread at the WUI may allow for the development of improved codes and standards, mitigation strategies, and numerical models to recreate events, which together will minimize the risks imposed by these fires [5].

Direct flame contact, radiation heat transfer, and the transport of firebrands are three recognized pathways from which fires spread from wildland vegetation into developed WUI communities [1]. Firebrands are small pieces of burning vegetation or structures (embers) that break off from combusting fuel and are transported by wind or fire-induced plumes to downwind locations, where the deposition of these firebrands onto different materials can lead to flaming or smoldering ignition. It has been shown that these firebrand “showers” are responsible for nearly half of the losses from investigated WUI fires [1, 6].

Firebrand generation studies have mostly focused on the mass and size distribution of firebrands generated from vegetative [6–10] and structural fuels [11, 12]. In a recent study by Hudson et al. [13], characteristics of firebrands generated from different tree species including the size distribution of firebrands and their number flux were reported. While these studies provide useful insights on the distribution of generated firebrands, they do not provide a firebrand yield expected from a particular vegetation or structural fuel under different ambient conditions hindering the development of numerical models for WUI fires. This is mostly because large-scale experiments are unable to collect all produced firebrands, instead relying on collection pans along the ground to collect some fraction of generated firebrands. Manzello et al. [10] measured firebrand production and employed mass loss rate profiles to measure the heat release rate of burning Korean pine and Douglas fir trees. In another study by the same authors, they presented the ratio of firebrand mass to total mass and mass loss during burning of Douglas fir and Korean pine trees [9]. A simultaneous measurement technique for gaseous and solid phase combustion products is ultimately needed, however, to link the burning rate of fuels to the mass of generated firebrands. Without this data and an associated carbon balance of product species to validate measurements, it is difficult to develop a numerical model of firebrand generation because the exact proportion of firebrands produced from specific fuels is unknown.

Some smaller-scale laboratory studies have been conducted to investigate the mechanisms by which firebrands are generated. Caton et al. [5] studied the breakage mechanism of thermally-degraded cylindrical wooden dowels, simulating smoldering firebrands, using three-point bending tests. Presenting a dimensional analysis, they discovered that the elastic strain of the dowels during loading impacted the strength and eventual fracture of these firebrands. This work followed a study by Barr and Ezekoye [14] which proposed a thermo-mechanical

breakage model from a hypothetical tree. Hudson and Blunck [15] developed a small-scale vertical wind tunnel which ignited sticks and Douglas fir branches, finding there is a critical diameter where branches break off, with diameter being the most important factor throughout this process.

This work presents a new wind tunnel platform capable of quantitatively characterizing various vegetative fuels found in the WUI under diverse environmental conditions. The setup has the capability to collect the majority of generated firebrands as well as major gaseous product species such as carbon dioxide (CO₂), carbon monoxide (CO) and oxygen (O₂), allowing for a total carbon balance, precise firebrand yield correlations, and heat-release rate calculations. Most numerical fire simulations, including the Fire Dynamics Simulator (FDS), rely on the heat-release rate to describe fire growth [16]. Therefore, an obvious method to initialize firebrands from these simulations is to relate the generation of firebrands to a time-dependent heat-release rate. While that is not fully accomplished here, a methodology to do so is established by performing a carbon mass balance to validate that this technique captures a large enough portion of solid and gaseous effluents to describe the mass burning process. Experiments in this study were conducted on branches from two fuels, Douglas fir and lodgepole pine, common conifers found in the United States. The presented tests point to the feasibility of this approach for additional fuels and serves as a useful baseline to initialize small-scale numerical models of firebrand transport.

2. Materials and Methods

A schematic of the experimental setup used to study the generation of firebrands from burning fuels is shown in Figure 1. The setup consisted of a 25 cm by 20 cm by 61 cm steel-walled wind tunnel in which different vegetative fuels ranging from small natural branches to wooden dowels could be burned. An opening of 15 cm by 15 cm at the top boundary of the wind tunnel with its center located 33 cm downstream of the tunnel entry provided access to the test section for deposition of fuels and measurement of the wind speed using a hot-wire anemometer. Additionally, two access ports with diameters of 2.5 cm located 7.5 cm and 20 cm downstream from the wind tunnel entry were provided for instrumentation and ignition of fuels. The opening at the top boundary as well as the access ports were sealed during the experiments to ensure a uniform air flow.

A variable-speed fan was utilized to generate wind in the test section ranging from 0.95 m/s at the lowest stable fan output to 4 m/s at its highest. The average peak wind speed at the center vertical location (10 cm) was seen to be 4.0 ± 0.1 m/s. Initial wind-speed measurements showed relatively uniform wind velocities in the axial and vertical directions in the test section, except for the points where the wind speed was near the peak of 4 m/s and for measurements performed near the walls, which were affected by expected boundary layer effects. Velocities could not be verified beyond the central test section or during experiments due to the design and hot gases generated during experiments. The average turbulence intensity based on velocity measurements at the centerline of the test

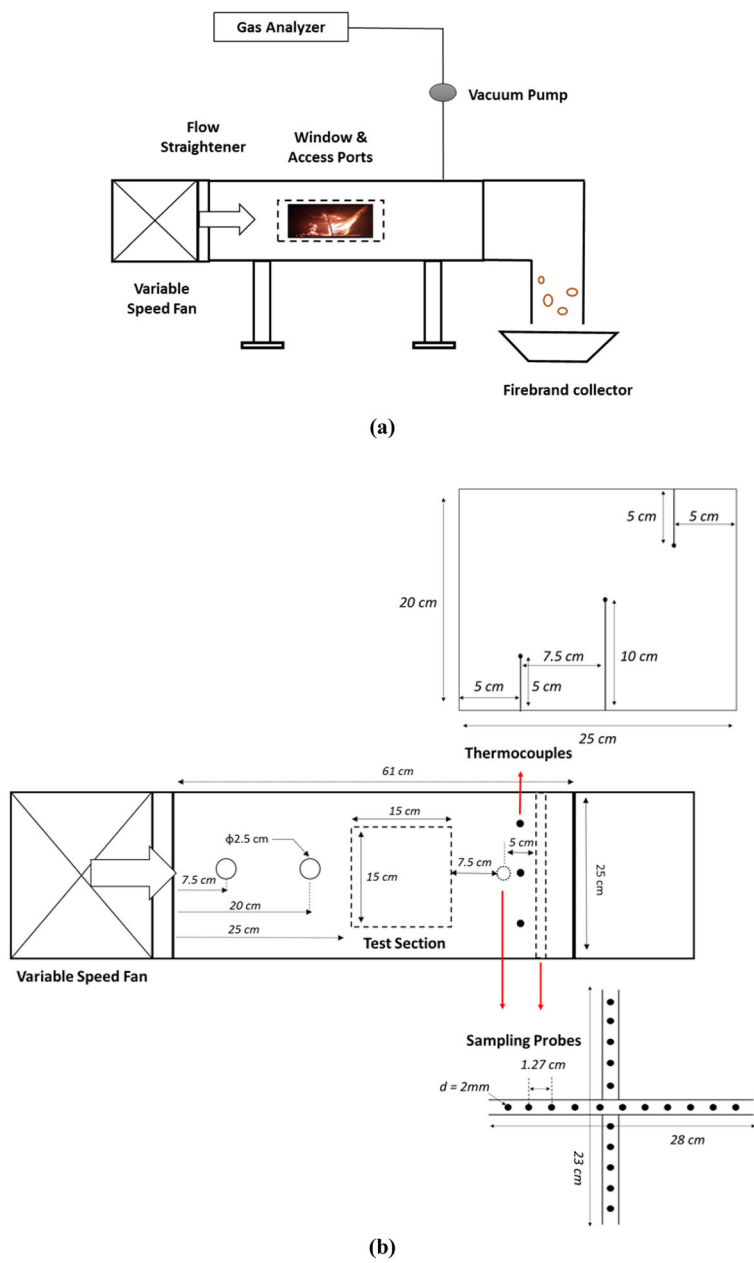


Figure 1. (a) Side-view schematic of the experimental setup designed to study generation of firebrands under different ambient conditions; (b) Top-view schematic of the wind tunnel: The setup includes a wind tunnel (middle), an array of K-type thermocouples (top right), sampling probes for gaseous species measurements (bottom right).

section and at different wind speeds was observed to be nearly 3%. Wind speed measurements at three vertical locations taken from the top edge of the wind tunnel centered along its width at the location of the test sample are shown in Figure 2. As can be seen in this figure, the velocities in the center of the tunnel are relatively uniform across a range of wind speeds. Optical access inside the wind tunnel was facilitated by an 18 cm by 8 cm window on the side of the tunnel to visualize the experiments using a camcorder. Downstream of the test section a 90-degree elbow was used to collect generated firebrands under which a pan filled with water was positioned to quench any collected glowing firebrands.

The wind tunnel included two metallic tubes with an array of small holes mounted perpendicular to one another 15 cm and 20 cm downwind of the center of the test section. These probes were employed to extract gaseous species from the downwind gases including CO₂, CO and O₂ using a gas analyzer (California Analytical Instruments, ZPA model). A particle filter and moisture absorbers were used upstream of the gas analyzer to prevent moisture and particulates from entering the sample lines with incoming gases. Given that the cross-sectional area of the wind tunnel was 25 cm by 20 cm, at the lowest wind speed of 0.95 m/s used in the experiments, this would translate to a volumetric flow rate of 47.5 l/s of air and effluents passing through the sampling probes for gaseous species measurements prior to collection of solid-phase firebrands, which occurred at the wind speed of 4 m/s corresponding to a volumetric flow rate of 200 l/s. Additionally, an array of three K-type thermocouples was used to measure the temperature of the downwind gases, where these thermocouples were positioned between the two sampling probes and their arrangement can be seen in Figure 1.

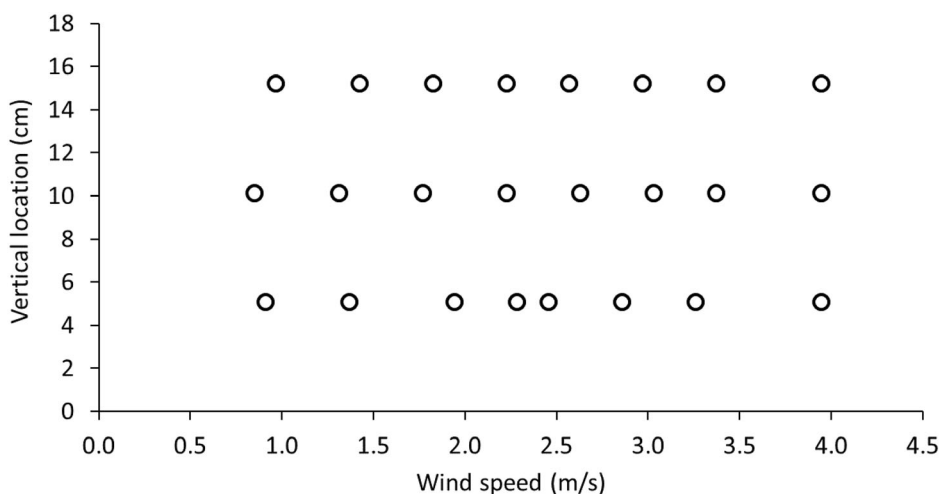


Figure 2. Wind speed measurements at three vertical locations taken from the top edge of the wind tunnel centered along its width at the location of the test sample. Results presented in this work were ignited at 0.95 m/s then run at 4 m/s.

The species concentration data as well as the temperatures were obtained using two separate data acquisition cards input to a National Instruments LabView program at a frequency of 10 Hz. Before each experiment, the gas analyzer was calibrated using nitrogen (N_2) gas which provided the zero concentration points for all the gases and a calibration gas containing 20% O_2 , 1% CO and 8% CO_2 , provided single points for calibration of each species using a linear function. An air baseline was also established during each series of experiments to account for the concentration of CO_2 , CO and O_2 in the ambient air. Additionally, temperatures of the downwind gases were measured with the three thermocouples and their average was employed to calculate gas properties in the calculations. The temperature and species data were obtained to ultimately calculate the masses of major product species, i.e. CO_2 , CO and O_2 , where the species data could also be used to account for heat-release rate.

In order to characterize the proportion of produced solid-phase firebrands vs. gaseous species, a simplified carbon balance is used to analyze experiments on small samples in the previously-described wind tunnel,

$$\begin{aligned} \text{Carbon in Fuel} = & \text{Carbon in } CO_2 + \text{Carbon in CO} + \text{Carbon in Firebrands} \\ & + \text{Carbon in Fuel Residue} \end{aligned} \quad (1)$$

assuming a negligible contribution of soot, unburned hydrocarbons, etc. Due to limitations of the experimental setup in this study for gaseous species measurements, only CO_2 , CO and O_2 could be measured. With regards to the negligible contribution of soot in the carbon mass balance, previous studies have shown that the emission factor (EF) of particulate matter (PM) is nearly two orders of magnitude lower than CO_2 and one order of magnitude than CO [17, 18]. Moreover, initial measurements in this study showed that the carbon production from soot was less than 0.2%; thus, the contribution of soot in the carbon balance was negligible compared to variability in fuel samples, etc.

Having obtained the mass of generated CO_2 and CO, Eqs. (2) to (4) can be utilized to account for the emission factor,

$$EF = \frac{\text{Mass of Product Species}[g]}{\text{Mass of Consumed Dry Fuel}[kg]} \quad (2)$$

and modified combustion efficiency (MCE),

$$MCE = \frac{\text{Mass of Carbon in } CO_2[g]}{\text{Mass of Carbon in } CO_2[g] + \text{Mass of Carbon in CO}[g]} \times 100 \quad (3)$$

while considering different Fuel Moisture Contents (FMC) [19],

$$m_{consumed} = \frac{m_{fuel}}{1 + FMC} - m_{residual} \quad (4)$$

In Eq. (4), after calculation of the mass of consumed fuel, its value was multiplied by the carbon content of the fuel to attain the total carbon content in the dry fuel. Additionally, FMC was measured using an AND moisture analyzer consisting of a quartz lamp and microbalance, where the reported FMC's were defined as

$$FMC = \frac{(\text{Mass of Wet Fuel} - \text{Mass of Dry Fuel})}{\text{Mass of Wet Fuel}} \quad (5)$$

Before starting the experiments with tree branches, a series of experiments with a propane-fueled (C_3H_8) Bunsen burner mounted inside the wind tunnel were performed to verify whether gaseous species attained a homogenous mixture for gaseous species sampling. This testing was key for characterization of the mass flow of generated CO_2 and CO , as good quality data was required to perform a mass balance and understand how much of the product species is constituted of gases compared to firebrands. During each experiment, the Bunsen burner was placed in the test section of the wind tunnel and the gaseous species concentrations were measured in the downstream flow for nearly three minutes. The average concentration of gases during the last 60 s of the experiments were used in calculation of the heat-release rate, employing an oxygen consumption method from White et al. [20]. Values from these experiments were compared to theoretical values of heat-release rate calculated using the fuel flow rates and considering the heat of combustion of 46 MJ/kg for propane [21]. While not ideal, a correction factor was implemented to account for poor mixing at some flow rates by comparing the values of heat-release rate between the experiments and theory, which was derived to be 0.76. This value was used to adjust the volumetric flow rate of the downwind gases in the mass calculations. Bunsen burner flames were purposefully set to a similar to flame length as the ones observed in firebrand generation experiments. It is true that the source is much more localized for a Bunsen burner flame, but a significant effect was not observed with varying heat release and at different wind speeds in this study. It is important to note the length of the tunnel was restricted so that generated firebrands are not destroyed or burned out in the process, so there is a careful balance requiring future re-designs.

Following the Bunsen burner experiments, lodgepole pine and Douglas fir branches obtained from the Missoula Fire Sciences Laboratory, Rocky Mountain Research Station, USDA Forest Service in Missoula, Montana were burned. Samples were approximately 10–15 cm in length, with the average diameter of the lodgepole pine and Douglas fir branches being 6.2 ± 1.9 mm and 2.9 ± 0.8 mm, respectively (with their uncertainty calculated using the Student t-test with a 95% confidence interval). Figure 3 shows pictures of lodgepole pine and Douglas fir samples used in the experiments. These samples were placed inside a laboratory convection oven at a temperature of 105°C until their moisture content reached below 5%. This was confirmed using the AND moisture analyzer, where the average moisture content of branches was seen to be 3% in this work. The mass of each single branch was measured before each experiment and the masses of its



Figure 3. Pictures of lodgepole pine (left) and Douglas fir (right) samples used in the experiments. A US Penny (19.05 mm diameter) is shown for scale.

residue, including any remaining needles or dowels that were collected after the experiments, were also measured.

After a series of experiments and initial analysis of their data, it was seen that the analysis would work best if the branches were ignited at a known value of air volumetric flow rate, where the lowest fan output resulting in a 0.95 m/s wind velocity was used for this purpose; however, ignition of branches under a windy condition was not feasible even when the branches had very low moisture content, as they would start smoldering soon after ignition leaving the branch almost completely unburned at the end of the experiments. Therefore, to enhance the ignition characteristics of these branches, 1.3 g of ethanol (C_2H_5OH) on average was sprayed on the branches before each experiment. Using ethanol resolved ignition issues and, given the well-known heat release characteristics of ethanol, it was seen to be easily implemented for the purpose of these experiments. The mass of generated gases from burning ethanol (small compared to test results) was later removed in the carbon balance of tested fuels in this study. The fuels were placed in the test section of the wind tunnel 33 cm downstream of the fan. The fuels were placed on a perforated steel plate which was used as a fuel holder. Ethanol was then sprayed on dry fuels, the fan was turned on until it reached a steady wind speed of 0.95 m/s, and then the branch and ethanol were ignited with a small butane lighter through a small access port upstream of the test section. Thus, the branches in each experiment were ignited under a 0.95 m/s wind speed and, after their transition from flaming to smoldering, the highest output of the fan yielding a wind speed of 4 m/s was applied on the branches. It was observed that the greatest mass of firebrands was generated at this highest wind velocity under which the experiments could be conducted.

Each experiment usually included burning three branches consecutively and, using the water-filled pan downwind of the tunnel, the generated firebrands from

each experiment were subsequently collected. The pan was then put in a convective oven at 105°C for nearly one day to ultimately obtain dry firebrands, where the mass of these embers was measured using a mass balance. Moreover, each experiment included the gaseous species concentration data as well as their temperatures, which were analyzed using a computer code producing mass generation profiles whose area under the curve were analyzed with the trapezoidal rule to obtain the final masses of CO₂ and CO produced after each experiment. The number of firebrand yield experiments were 12 and 10 for lodgepole pine and Douglas fir branches, respectively. Additionally, the number of experiments run to calculate a carbon balance for Douglas fir branches, as discussed in [Sect. 3.3](#), were 8.

3. Results

3.1. Generated Firebrands

Figure 4 displays a sequence of images of a Douglas fir branch before and after an experiment. As shown in this figure, the Douglas fir branch was ignited at image sequence 1, where the wind speed was 0.95 m/s. The wind speed stayed the same until image sequence 8, where it was increased to 4 m/s until the end of the experiment. The role of fuel species size and diameter in generation of firebrands has been highlighted in previous works [22, 23]. Thus, images of the branches were taken before and after the experiment to investigate the role of branch size and diameter in generation of firebrands at the defined conditions for the experiments. The Douglas fir branches had a diameter of approximately 2.9 mm, where after the experiment the whole branch was nearly consumed. The small part of the branch which was unburned after the experiment could be due to a suboptimal ignition system or near-wall effects, which can be improved in future works. Additionally, although the diameter of branches plays an important role in the amount of generated firebrands, this effect was not particularly investigated in this study as the focus of this work was to demonstrate the capabilities of the new experimental setup rather than performing a factorial analysis; nonetheless, this warrants further investigation and can be incorporated in future works.

Figures 5 and 6 show the mass of generated firebrands in terms of initial mass of branches and the firebrand yield in terms of initial mass of branches for dried lodgepole pine and Douglas fir, respectively. Results were all conducted at the highest wind speed (4 m/s). Firebrand yield in this study was defined as the ratio of the mass of firebrands over the initial (dry) mass of branches. As can be seen in this figure, there is an increase in the mass of generated firebrands with an increase in the initial mass of the fuel sample. A simple linear function was utilized to represent a correlation between mass of the fuel and mass of firebrands at the conditions tested.

A linear fit to the data in Figures 5a and 6a demonstrates a slight increase in the mass of generated firebrands. As can be seen in Figures 5a and 6a, the values of R^2 are 0.72 and 0.22, respectively. R^2 indicates the goodness of fit for the fitted line following the mass of generated firebrands versus the mass of fuels in this study. A higher R^2 achieved for lodgepole pine branches (Figure 5a) shows that a

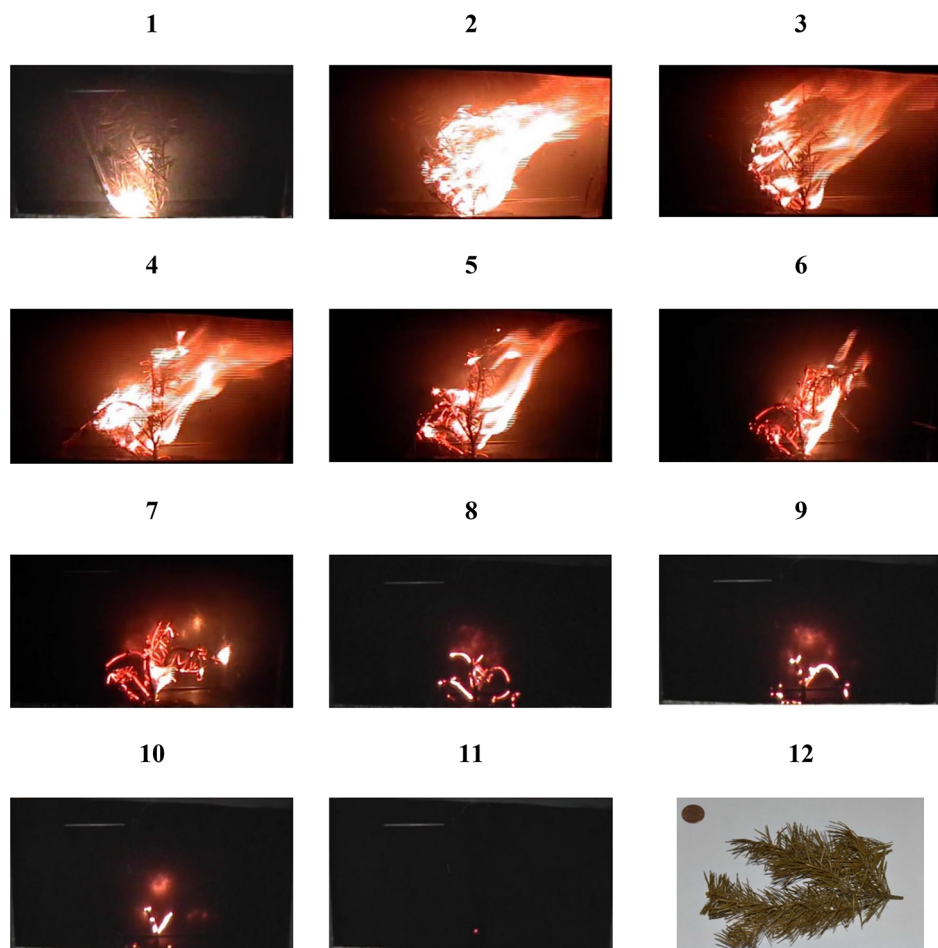


Figure 4. A sequence of images of a burning Douglas fir branch exposed to an initial wind velocity of 0.95 m/s until image sequence 8 where it was increased to 4 m/s for the rest of the experiment. Frame 12 shows an image of the branch before an experiment. A US Penny is shown for scale.

better fit was achieved for lodgepole pine branches compared to Douglas fir branches, which translates into a lower scatter of data for lodgepole pine branches. The rather poor fit for Douglas fir branches in Figure 6a demonstrates the necessity of acquiring more data and further investigation into the mass of generated firebrands based on the mass of burned Douglas fir. Firebrand yield also shows a slight increasing trend as the initial mass of the fuel increases for lodgepole pine branches (Figure 5b); however, what appears to be a slight decrease or constant value of firebrand yield is observed for Douglas fir branches (Figure 6b) when its initial mass is increased. Any trend line applied here achieves a poor degree of fit

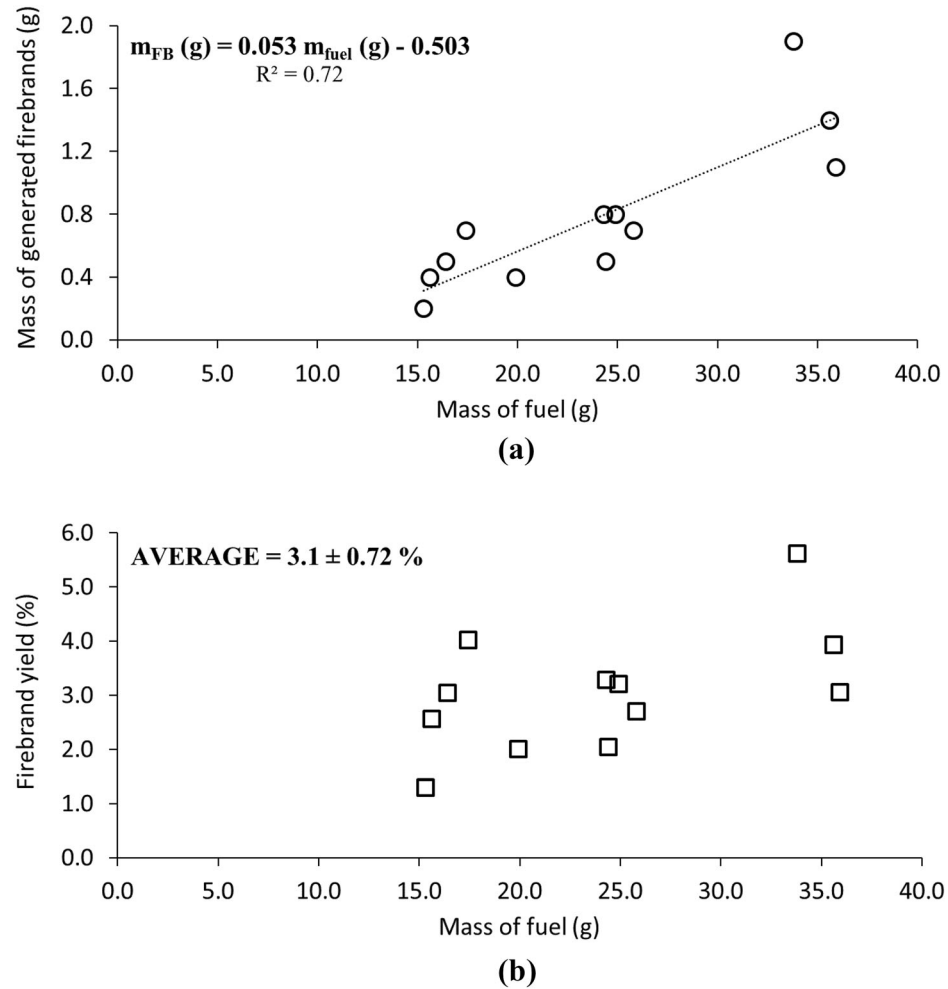


Figure 5. (a) Mass of generated firebrands from lodgepole pine branches in terms of initial mass of dry lodgepole pine samples; (b) Firebrand yield in terms of initial mass of dry lodgepole pine samples.

due to natural scatter in the data; therefore, they are not shown on these graphs and future experiments are required to confirm the trends at different scales. An average firebrand yield for lodgepole pine and Douglas fir branches can be resolved, including its uncertainty calculated utilizing the Student's t-test method with a 95% confidence interval. This was seen to be $3.1 \pm 0.72\%$ and $3.9 \pm 0.91\%$, respectively. It is certainly possible that this could change with scale, notably due to changes in branch diameter; however, our methodology could be used to test this at increasing scales in the future.

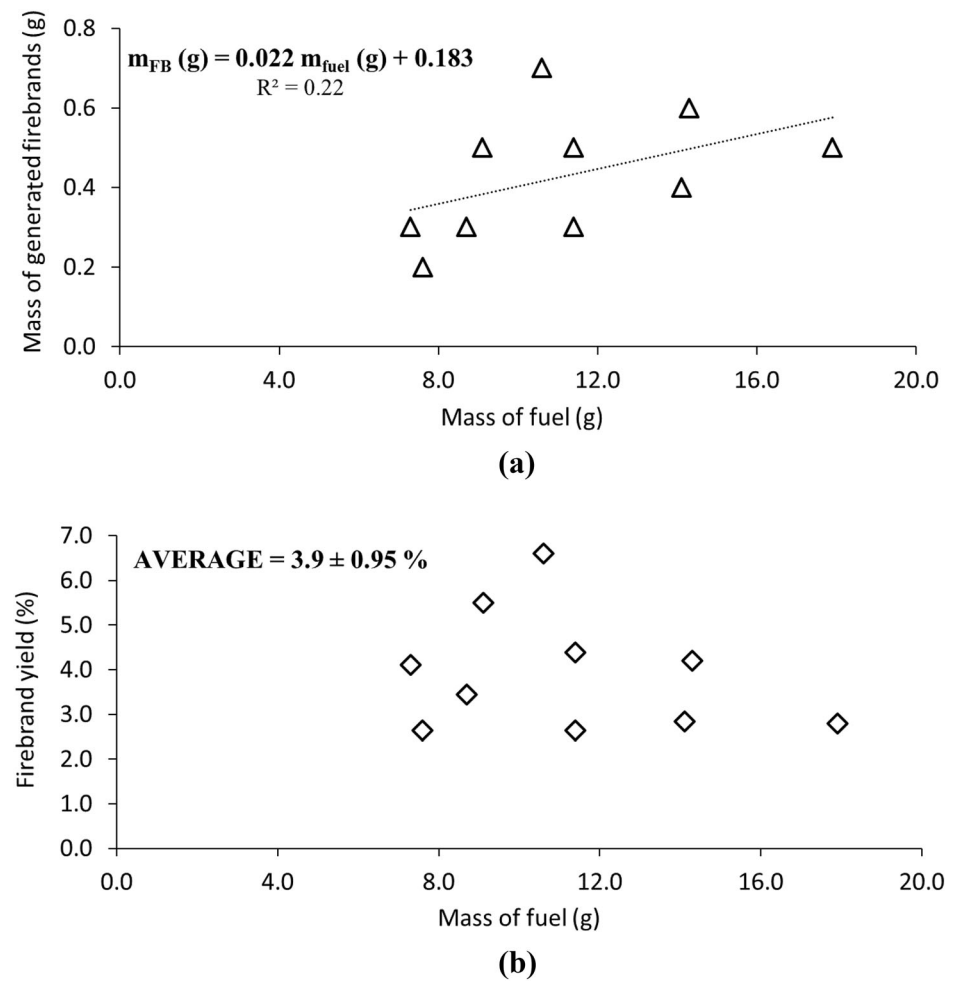
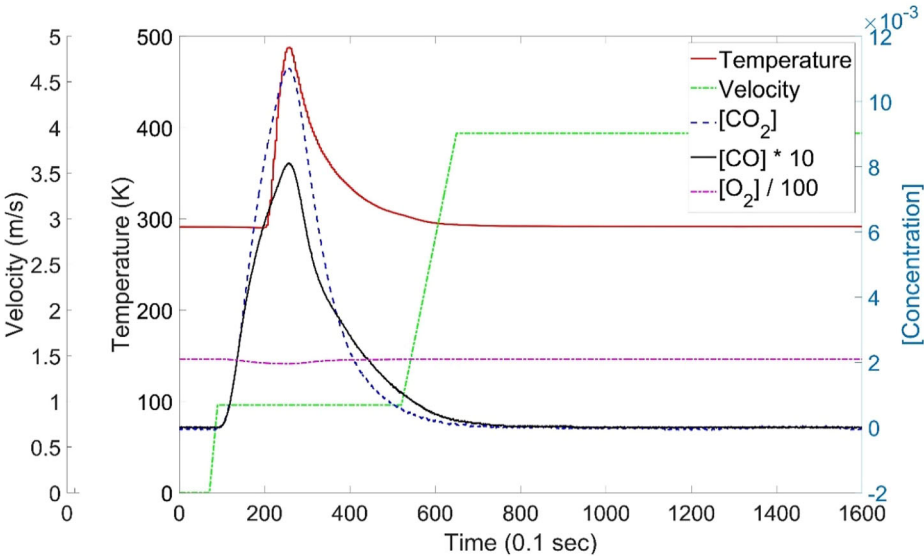


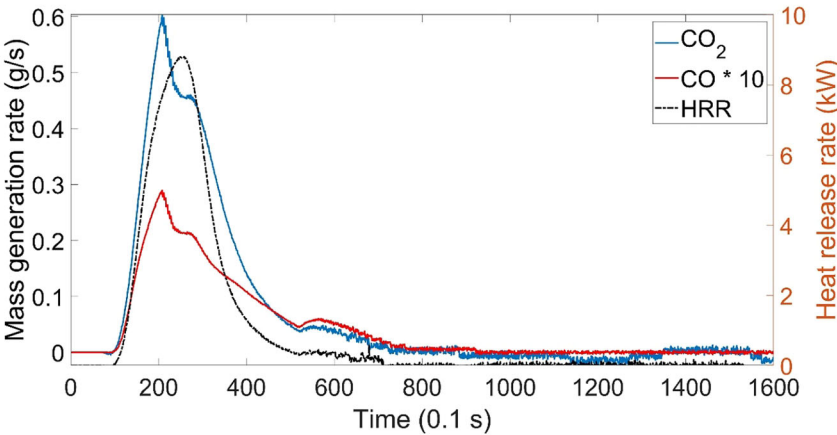
Figure 6. (a) Mass of generated firebrands from Douglas fir branches in terms of initial mass of dry Douglas fir samples; (b) Firebrand yield in terms of initial mass of dry Douglas fir samples.

3.2. Gaseous Species Concentration and Temperature Profiles

Figure 7a displays an example of collected profiles of temperature, velocity and concentrations of CO₂, CO and O₂ for one test. The profiles of CO and O₂ have been multiplied by 10 and divided by 100, respectively, to show all the values with the same scale. Note the velocity was measured during cold-flow tests and a linear fit was applied between average wind speeds measured during the ramp-up period of the blower fan. Knowing the concentration of gases as well as the temperature-dependent density, the masses of the produced gases were calculated. Figure 7b demonstrates the mass generation profiles of CO₂ and CO as well as the temporal evolution of heat-release rate from the same branch discussed in Figure 7a. Anal-



(a)



(b)

Figure 7. (a) Profiles of temperature, wind velocity as well as concentration of gaseous species for a single Douglas fir branch; (b) Mass generation profiles of CO_2 and CO as well as heat release rate as a function of time for a single Douglas fir branch.

ogous to Figure 7a, the profile of CO in Figure 7b has been multiplied by 10 to show all the values on the same scale. These calculated masses were later utilized in a carbon balance to understand the percentage of produced gases versus firebrands. In these figures, a Douglas fir branch with a mass of 6.8 g along with 1.3 g of ethanol was burned, resulting in 8.51 g and 0.70 g of generated CO_2 of

CO from the branch, respectively. These calculations were performed for each branch in all experiments.

Calculations of heat-release rate were performed utilizing the measured concentrations of CO₂, CO and O₂ in each experiment. As was mentioned earlier, these calculations were performed using the O₂ consumption calorimetry method from White et al. [20]. The area under the curve represents the net heat release; thus, considering net heats of combustions of 19.6 MJ/kg and 26.81 MJ/kg for Douglas fir and ethanol [21], respectively, the net heat release from theory was calculated to be 148.5 kJ and from the experiments, it was observed that the heat release had a value of 149.6 kJ using the method from White et al. [20].

3.3. Carbon Balance

Based on a study by McMeeking et al. [19], the carbon content of lodgepole pine and Douglas fir was reported to be between 42–50%, and 54%, respectively. Additionally, it was assumed that the whole mass of remaining firebrands is constituted of carbon. As was mentioned earlier, Eq. (1) was employed to investigate if the carbon balance holds true for the experiments and, based on that, how much of the carbon comes from major product gases, namely CO₂ and CO, compared to firebrands. Consumed carbon in Figure 8 represents the carbon in the initial fuel subtracted by the carbon in the fuel residue, and the y-axis in Figure 8 represents only the generated carbon from the measured product gases, i.e. CO₂ and CO. A linear trend line was fitted to the data and as can be observed in this figure, higher carbon content in branches resulted in higher generated carbon in the form of gases. Additionally, based on Eqs. (2) to (4), the average modified combustion efficiency of the burned Douglas fir branches as well as emission factors for CO₂ and CO generated from these branches and their uncertainty was calculated to be $90.3 \pm 1.9\%$, 1377 ± 188 (g kg⁻¹) and 93.8 ± 14.3 (g kg⁻¹),

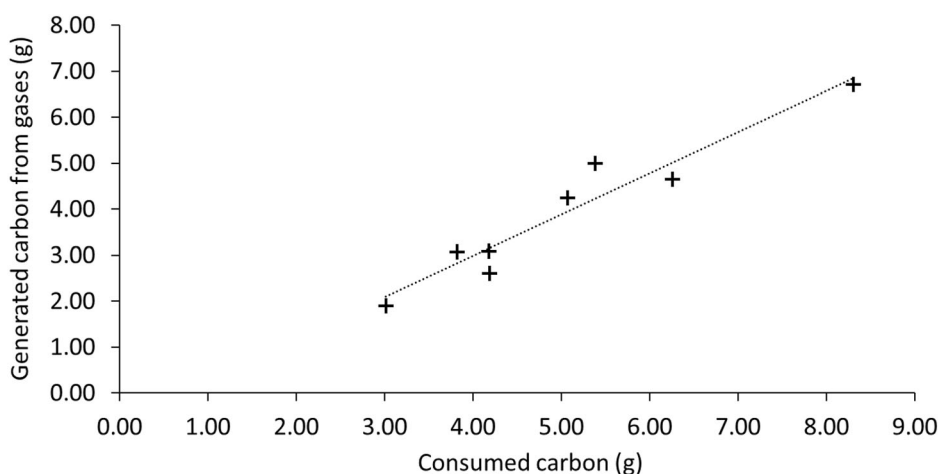


Figure 8. Generated carbon from gases in terms of consumed carbon in dry Douglas fir branches.

respectively. Table 1 shows the detailed values from the carbon mass balance for Douglas fir branches corresponding to Figure 8. Only two significant figures are shown due to the inherent variability in these values. It should be noted that in one of the experiments where the initial fuel mass was 11.4 g, the amount of consumed carbon is nearly equal to the produced carbon from the gases and firebrands. Given the fact that some of the product species could be lost during each experiment, these values reflect some of the uncertainties in the results of the carbon mass balance, which warrants further investigation in future works.

4. Discussion

The experiments in this work have shown the feasibility of collecting data on masses of generated firebrands and gaseous products from small branch samples in the laboratory. Data presented from dry lodgepole pine and Douglas fir samples at a wind velocity of 4 m/s reveals that a relatively low mass yield, 3.1% and 3.9%, respectively, is generated from the initial mass of the branches at the tested scale. Higher firebrand yield in the Douglas fir branches compared to the lodgepole pine branches under the same moisture content and wind conditions could be attributed to the smaller branch diameters of the Douglas fir used in this study. Additionally, linear correlations represented in Figures 5 and 6 are the firebrand production correlations obtained in this work. These types of correlations are key in characterization of the amount of firebrands generated from different species under different ambient conditions. The methodology presented in this work can easily be extrapolated to larger masses of trees and branches under the same conditions provided a larger apparatus is used. However, the correlations presented in this work are only a means to give an approximate baseline of the mass of generated firebrands from burning these fuels at the specified experimental conditions in this study. Caution should be applied when employing these correlations outside of the range of performed experiments in this research. More experiments at

Table 1
Detailed Values of Carbon Mass Balance for Douglas Fir Branches

Initial fuel mass (g)	Mass of fuel residue (g)	Consumed carbon (g)	Carbon from firebrands (g)	Carbon from CO ₂ (g)	Carbon from CO (g)
14.3	4.5	5.1	0.6	3.8	0.5
11.4	4.0	3.8	0.3	2.8	0.3
17.9	2.0	8.3	0.5	6.0	0.7
11.4	1.1	5.4	0.5	4.7	0.3
8.7	0.7	4.2	0.3	2.3	0.3
14.1	2.1	6.3	0.4	4.2	0.5
7.6	1.8	3.0	0.2	1.7	0.2
9.1	1.1	4.2	0.5	2.8	0.3

increasing scales are required to allow for a comprehensive correlation of fire-brand generation, which warrants investigation in future works.

Comparing the area under the curve from heat release rate plots of the tested branches with the theoretical values of heat release revealed that the average heat release from experiments and theory for Douglas fir were seen to be 77 kJ and 93 kJ, respectively, having a difference of 27%. While the results for lodgepole pine branches were limited, it was observed the values of heat release from experiments and theory for these branches were 103 kJ and 174 kJ, respectively, with a difference of 36%. It should be noted that ethanol was used in the experiments to enhance ignition and since the experiments were carried out right after ethanol was sprayed on the branches, this would eventually minimize the effect of ethanol evaporation on the obtained results. Furthermore, since the profiles of downstream gases were used to calculate the heat release rate, the values of heat release in this study include the emissions from burning ethanol as well; nonetheless, because of complete combustion of ethanol where it only transitioned to CO₂ and produced no CO and due to the fact that only a small amount of ethanol was utilized during the course of the experiments, it is safe to assume that the calculated value of heat release were mostly from the branches. Additionally, the carbon mass balance was not satisfied in a few experiments, which was seen to be due to uncertainties in the measured gas concentrations and hence, these experiments were excluded from the carbon mass balance analysis.

The observed trend in Figure 8 is analogous to what was reported in McMeeking et al. [19] for a variety of species including Douglas fir, where they also saw a nearly linear relationship between the emitted carbon from product species and the consumed carbon in the fuel. It has been argued in their work that since the mass of emitted carbon is highly correlated with the mass of consumed carbon, as is the case in this study ($R^2 = 0.92$ compared to $R^2 = 0.96$ in McMeeking et al. [19]), the extractive species sampling method could be assumed to be operating under well-mixed conditions. Thus, the gaseous species collection system in the wind tunnel facility in this work, albeit far from ideal, has successfully captured the majority of the gaseous product species. Additionally, calculating the ratio between produced carbon (in the form gaseous species as well as firebrands) and consumed carbon, it was seen that on average $76.4 \pm 8.6\%$ were in the form of gases and $8.4 \pm 2.0\%$ were in the form of firebrands. This shows that approximately 15.2% were not captured by system, either due to limitations of the gas analyzer in measuring carbon from C₂ – C₄ hydrocarbons, organic compounds, elemental carbon, particulates etc., or loss of product species in the experiments mainly in the form of ash, unburned fuel as well as unmeasured CO₂ and CO.

The average combustion efficiency of dry Douglas fir branches in this study was calculated to be $90.3 \pm 1.9\%$, and the average emission factors for CO₂ and CO were seen to be 1377 ± 188 (g kg⁻¹) and 93.8 ± 14.3 (g kg⁻¹). Comparing to the work of McMeeking et al. [19], where the reported values for the combustion efficiency and the emission factors of CO₂ and CO for dry Douglas fir were calculated to be $90.6 \pm 3.6\%$, 1579 ± 193 (g kg⁻¹) and 106.8 ± 32.4 (g kg⁻¹), respectively, there is a good agreement between the combustion efficiency and the emission factors of CO₂ and CO within the calculated uncertainty in both works.

5. Conclusions

A wind tunnel facility, capable of simulating wildland fires at small scale and at different ambient conditions, was developed to investigate and quantify the generation of firebrands from different fuels. Experiments on vegetative fuels including dry lodgepole pine and Douglas fir branches at a wind speed of 4 m/s were performed and it was observed that the firebrand yield for these species under the aforementioned experimental conditions were nearly 3% and 4%, respectively. Important correlations representing the mass of generated firebrands in terms of initial mass of fuels were derived, and the presented methodology could be easily used in the future to estimate the mass of generated firebrands at higher fuel masses and in a real wildfire scenario. The setup also enabled measurement of downstream gaseous species concentrations, allowing for calculation of heat-release rate, which together with masses of produced firebrands can provide significant validation targets for model development. A carbon mass balance was utilized to understand the mass of generated firebrands vs. gases after each set of experiments, and it was proposed that the time-dependent heat release rate can be coupled to firebrand yield, providing data for development and validation of numerical models. While that is not fully accomplished here, the methodology is established by performing a mass balance to validate that the technique captures enough solid and gaseous effluents to describe the mass burning process.

The presented experimental setup in this study along with the obtained results, albeit limited to a small experimental range, have introduced a new and unique pathway for characterization of firebrand generation from WUI fuels. Although the experiments were performed at small-scale, the methodology developed in this study can be scaled up to a full-scale experiment representative of a real wildland fire scenario. The current experimental setup has some limitations and before providing final answers to the firebrand generation problem, future work is required which should include modifications to the experimental setup to expand the range of experimental conditions with more repetitions, higher fuel mass, larger sample sizes and on different fuel species, which all together could provide valuable simple multi-variable correlations for quantification of firebrand production at different ambient conditions.

Acknowledgements

This work was supported by the National Institute of Standards and Technology (NIST) under award number # 60NANB18D243. The authors would like to thank Ben Biallas, Xingyu Ren, and Sriram Bharath Hariharan for their help in experimentation as well as instrumentation and Chelsea Phillips and Sara McAllister from the USDA Forest Service for acquiring fuels. MG would also like to thank Kevin McGrattan, who suggested the current line of work, as well as Kathryn Butler, Kuldeep Prasad, Randy McDermott, Isaac Leventon, Samuel Manzello, Jiann Yang, and Nelson Bryner for their support and advice throughout the course of this project.

Declarations

Conflict of interest The authors declares that they have no conflict of interest.

References

1. Caton SE, Hakes RSP, Gorham DJ, Zhou A, Gollner MJ (2017) Review of pathways for building fire spread in the wildland urban interface part i: exposure conditions. *Fire Technol* 53:429–473. <https://doi.org/10.1007/s10694-016-0589-z>
2. Hakes R, Caton S, Gorham DJ, Gollner MJ (2016) A review of pathways to building fire spread in the wildland urban interface part ii: response of components and systems and mitigation strategies in the united states. *Fire Technol* 53:475–515
3. Manzello SL, Suzuki S, Gollner MJ, Fernandez-Pello AC (2020) Role of firebrand combustion in large outdoor fire spread. *Prog Energy Combust Sci* 76:100801. <https://doi.org/10.1016/j.peccs.2019.100801>
4. Syifa M, Panahi M, Lee CW (2020) Mapping of post-wildfire burned area using a hybrid algorithm and satellite data: the case of the camp fire wildfire in California, USA. *Remote Sens* 12(4):623. <https://doi.org/10.3390/rs12040623>
5. Caton-Kerr SE, Tohidi A, Gollner MJ (2019) Firebrand generation from thermally-degraded cylindrical wooden dowels. *Front Mech Eng* 5:1–12. <https://doi.org/10.3389/fmech.2019.00032>
6. Manzello SL, Cleary TG, Shields JR, Maranghides A, Mell W, Yang JC (2008) Experimental investigation of firebrands: generation and ignition of fuel beds. *Fire Saf J* 43:226–233. <https://doi.org/10.1016/j.firesaf.2006.06.010>
7. Manzello SL, Maranghides A, Mell WE, Cleary TG, Yang JC (2006) Firebrand production from burning vegetation. *For Ecol Manage* 234:S119. <https://doi.org/10.1016/j.foreco.2006.08.160>
8. Mell W, Maranghides A, McDermott R, Manzello SL (2009) Numerical simulation and experiments of burning douglas fir trees. *Combust Flame* 156:2023–2041. <https://doi.org/10.1016/j.combustflame.2009.06.015>
9. Manzello SL, Maranghides A, Shields JR, Mell WE, Hayashi Y, Nii D (2009) Mass and size distribution of firebrands generated from burning Korean pine (*Pinus koraiensis*) trees. *Fire Mater* 33:21–31
10. Manzello SL, Maranghides A, Shields JR, Mell WE, Hayashi Y, Nii D (2007) Measurement of firebrand production and heat release rate (HRR) from burning Korean pine trees. *Proc 7th AOSFST*. <https://iafss.org/publications/aofst/7/108>
11. Suzuki S, Manzello SL, Hayashi Y (2012) The size and mass distribution of firebrands collected from ignited building components exposed to wind. *Proc Combust Inst* 34:2479–2485
12. Suzuki S, Manzello SL, Lage M, Laing G (2012) Firebrand generation data obtained from a full-scale structure burn. *Int J Wildl Fire* 21:961–968
13. Hudson TR, Bray RB, Blunck DL, Page W, Butler B (2020) Effects of fuel morphology on ember generation characteristics at the tree scale. *Int J Wildl Fire* 29(11):1042–1051
14. Barr BW, Ezekoye OA (2013) Thermo-mechanical modeling of firebrand breakage on a fractal tree. *Proc Combust Inst* 34:2649–2656. <https://doi.org/10.1016/j.proci.2012.07.066>

15. Hudson TR, Blunck DL (2019) Effects of fuel characteristics on ember generation characteristics at branch-scales. *Int J Wildl Fire* 28:941–950. <https://doi.org/10.1071/WF19075>
16. McGrattan K, Hostikka S, McDermott R, Floyd J, Weinschenk C, Overhold K (2020) Sixth Edition Fire Dynamics Simulator User's Guide (FDS). NIST Spec Publ 1019 Sixth Edit: <https://doi.org/https://doi.org/10.6028/NIST.SP.1019>
17. Hariharan SB (2020) Experimental Investigations and Scaling Analyses of Whirling Flames. PhD Dissertation, University of Maryland, College Park
18. Urbanski S (2014) Wildland fire emissions, carbon, and climate: Emission factors. *For Ecol Manage* 317:51–60
19. McMeeking GR, Kreidenweis SM, Baker S et al (2009) Emissions of trace gases and aerosols during the open combustion of biomass in the laboratory. *J Geophys Res Atmos* 114:1–20. <https://doi.org/10.1029/2009JD011836>
20. White JP, Link ED, Trouvé A, Sunderland PB, Marshall AW (2017) A general calorimetry framework for measurement of combustion efficiency in a suppressed turbulent line fire. *Fire Saf J* 92:164–176. <https://doi.org/10.1016/j.firesaf.2017.06.009>
21. Drysdale D (2016) *SFPE Handbook of Fire Protection Engineering*, Chapter 5. Springer, Fifth Edit
22. Thomas JC, Mueller EV, Santamaria S et al (2017) Investigation of firebrand generation from an experimental fire: development of a reliable data collection methodology. *Fire Saf J* 91:864–871. <https://doi.org/10.1016/j.firesaf.2017.04.002>
23. El Houssami M, Mueller E, Filkov A, Thomas JC, Skowronski N, Gallagher MR, Clark K, Kremens R, Simeoni A (2016) Experimental procedures characterising firebrand generation in wildland fires. *Fire Technol* 52:731–751

Publisher's Note Springer Nature remains neutral with regard to jurisdictional claims in published maps and institutional affiliations.